

Title:

**DETERMINING ELECTRO-OPTIC COEFFICIENTS
FOR LITHIUM TANTALATE USING AN ELECTRO-
OPTIC SCANNING DEVICE**

Author(s):

Joanna L. Casson, Kevin T. Gahagan,
David A. Scrymgeour, Ravinder K. Jain,
Jeanne M. Robinson, Venkatraman Gopalanc

Submitted to:

<http://lib-www.lanl.gov/la-pubs/00796262.pdf>

DETERMINING ELECTRO-OPTIC COEFFICIENTS FOR LITHIUM TANTALATE USING AN ELECTRO-OPTIC SCANNING DEVICE

Joanna L. Casson^{a,b}, Kevin T. Gahagan^a, David A. Scrymgeour^c, Ravinder K. Jain^b,
Jeanne M. Robinson^a, Venkatraman Gopalan^c

^aChemistry Division, Los Alamos National Laboratory, Los Alamos, NM, 87545¹

^bCenter for High Technology Materials, University of New Mexico, Albuquerque, NM 87106²

^cMaterials Research Laboratory, Pennsylvania State University, State College, PA 16802³

ABSTRACT

We demonstrate a ferroelectric optical device based on single crystal LiTaO₃ that can scan a laser beam from the visible to the infrared. It utilizes the electro-optic effect in the ferroelectric that has potentially high intrinsic response times of GHz. There are many applications to such scanning devices in the infrared such as optical switching, spectrometry, microscopy, and sensing.

Lithium tantalate has two ferroelectric polarization states that are antiparallel (180°) to each other. The domain states can be reversed by applying an electric field of ~21 kV/mm at room temperature. By reversing the domain structure in the crystal, we can create domains in the crystal of almost any desired shape. By creating prism-shaped domain, we can create a ferroelectric deflector or scanner by applying either static or sweeping voltages across the crystal. This scanner is capable of scanning wavelengths from 0.4-5 μm. The scanning performance varied from a total deflection angle of 13.38° at 1558 nm to 16.18° at 632.8 nm. Since the amount of deflection of the incoming light is determined by the applied voltage, the electro-optic coefficient and other fixed quantities, by measuring the deflection angle as a function of wavelength, the dispersion of the electro-optic coefficient in lithium tantalate can be determined.

In these experiments, the scanner was characterized from the visible (632.8 nm) to mid-infrared (1558 nm). Both extraordinary and the ordinary polarizations of light were used, in order to determine the electro-optic coefficients, r_{33} and r_{31} . Except for the values at 632.8 nm, these values of the electro-optic coefficients have not been previously reported. For lithium tantalate, r_{33} at 632.8 nm is reported in the literature as 30.2 pm/V. We found that this decreases to 27.1 pm/V at 1558 nm. For the extraordinary polarization, r_{13} varied from 7.55 pm/V (632.8 nm) to 6.84 pm/V (1558 nm).

¹ JLC: 505-665-6186 (voice), 505-667-4418 (fax), email: casson@lanl.gov; KTG: 607-248-1165 (voice), email: gahagankt@corning.com
JMR: 505-665-4834 (voice), 505-667-4418 (fax), email: jeanne.robinson@lanl.gov

² RKJ: 505-272-7842 (voice), email: jain@chtm.unm.edu

³ DAS: (814) 865-0497 (voice), email: das251@psu.edu; VG: (814) 865-2910 (voice), email: vgopalan@psu.edu

INTRODUCTION

We demonstrate a ferroelectric optical device based on single crystal LiTaO_3 that can scan a laser beam from the visible to the infrared. Integrated micro-optical devices based in ferroelectric materials offer advantages for applications such as optical switching, spectrometry, microscopy, and sensing. Further, other devices, such as tunable electro-optic lenses, and gratings are easily integrated into the device [1-6]. The rapid intrinsic electro-optic response (GHz) and minimal leakage current (nanoamps) of these materials allow efficient high-speed operation in comparison with mechanical or liquid crystal devices.

Lithium tantalate and lithium niobate are ideal materials for infrared scanning devices, since LiNbO_3 is transparent from 0.4-4 μm wavelengths and lithium tantalate extends this range up to a wavelength of 5 μm . These materials display excellent electro-optic properties [7], low refractive index dispersion in infrared [8], and low light propagation losses [8]. They are also available as high quality, optical-grade, single-crystal wafers which are relatively inexpensive. Both materials have two ferroelectric polarization states that are antiparallel (180°) to each other. Their domain states can be reversed by applying an electric field of ~ 21 kV/mm at room temperature [9]. By reversing the domain structure in the crystal, we can create domains in the crystal of almost any desired shape.

Both lithium tantalate and lithium niobate are uniaxial crystals with 3m point group symmetry and ferroelectric polarization in the uniaxial z -direction. Consider a z -polarized light beam propagating through a z -cut LiTaO_3 wafer in the x - y plane, and an external electric field, E_3 , applied in the z -direction. The electro-optic effect gives rise to an index change

$$\Delta n_e = -\frac{1}{2} n_e^3 r_{33} E_3, \text{ where } n_e \text{ is the extraordinary refractive index, and } r_{33} \text{ is the electro-optic}$$

coefficient. For ordinary polarized light, $\Delta n_o = -\frac{1}{2} n_o^3 r_{13} E_3$, where n_o is the ordinary refractive index. If the electric field is parallel (or antiparallel) to the spontaneous ferroelectric polarization, then Δn is negative (or positive). At a 180° domain boundary, the light encounters a refractive index change of $2\Delta n_e$ for extraordinary light and $2\Delta n_o$ for ordinary polarized light. The electro-optic scanner described here was based on a horn-shaped scanner design as detailed elsewhere [10]. Figure 1 shows a Beam Propagation Method (BPM) simulation of the designed scanner.

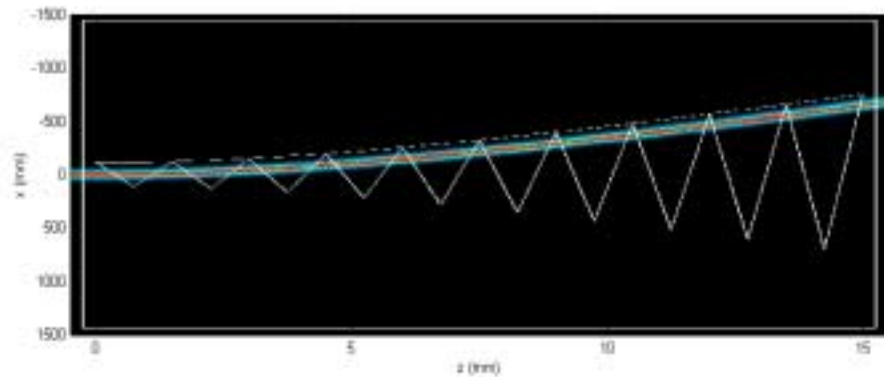


FIGURE 1: Beam Propagation Method simulation of horn-shaped scanner in Lithium Tantalate operating at 15 kV/mm for an ordinary polarized light beam.

For an electric field E_3 of ± 15 kV/mm, the simulation shows a predicted scan angle of $\pm 8.2^\circ$ at 632.8 nm. This corresponds to a deflection angle of 33.2 mrad/kV. In the simulation, an electro-optic coefficient of $r_{33}=30.5$ pm/V and a refractive index of 2.180 was used at this wavelength [8].

METHODS

The deflection angle of the electro-optic scanner was characterized at four different wavelengths, 632.8 nm (He-Ne), 980 nm (Ti-Sapphire), 1330 nm (diode) and 1558 nm (diode). The experimental set-up is shown in Figure 2.

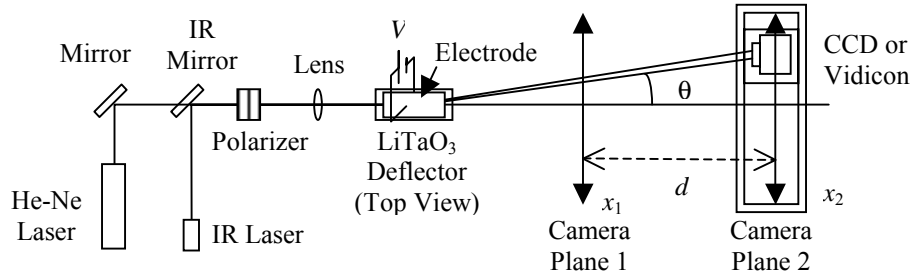


FIGURE 2: Schematic of the electro-optic scanner characterization set-up. IR lasers used are a Ti-Sapphire at 980 nm and fiber-coupled diodes at 1330 nm and 1558 nm.

The scanning performance of the device is determined by applying a voltage to the crystal from -4.3 kV to $+4.3$ kV. The lateral displacement of the beam is measured by a charge coupled device (CCD) (for 632.8 nm, 980 nm and 1330 nm) or a vidicon camera (for 1550 nm). At zero applied volts, the beam centroid is centered in the camera's field of view. As voltage is applied at discrete values, the camera is moved with a high-precision translation stage until the beam centroid is once again centered in the camera. From the measured beam displacement at two different image planes, the angular deflection at each voltage can be determined as: $\theta(V) = \tan^{-1}[(x_2(V) - x_1(V))/d]$, where V is the applied voltage, x_1 is the displacement at the near plane, x_2 is the displacement at the far plane, and d is the distance between the two planes. Table I lists the wavelength dependence of the angle of deflection for both ordinary and extraordinary polarized input beams. The reduction in the deflection angle per unit field at longer wavelengths is a direct result of lower refractive index, and lower electro-optic coefficient for LiTaO₃ with increasing wavelength in the infrared. The index dispersion with wavelength is reported in literature [8]. We describe below how one can extract the dispersion in the electro-optic coefficients with wavelength.

The device was fabricated on a 286 μm thick, single crystal wafer of z-cut LiTaO₃. Starting from a single domain wafer, ferroelectric domains were patterned in the shape of prisms comprising the horn-shaped scanner shown in Fig. 1. This was done by electric field induced domain inversion using lithographically patterned electrodes as described in detail elsewhere [11,12]. Finally uniform electrodes were deposited on both sides of the wafer, and the device tested as described below.

RESULTS AND DISCUSSION

We also found that there was a slight convex curvature on the back face of the crystal. This curvature, which most likely resulted from the hand polishing of the crystal face, decreases the measured deflection angle from that predicted by the BPM simulations. With careful measurements of the curvature, it is possible to correct the data for direct comparison with BPM simulations that assume a flat back surface.

To determine the magnitude of the curvature, a laser beam was reflected off the front surface. The position of the reflected beam was measured as the crystal was translated in a direction parallel to the crystal face. The displacement of the reflected beam is proportional to the slope of the surface. By integrating across the surface, the surface curvature is computed from the measured slopes. The radius of curvature was determined to be 810 ± 40 mm. The effect of the curvature is to reduce the expected scan angle by $\sim 1\%$ in comparison with a flat surface. For accuracy, we have included a correction for this curvature in the data in Table I.

TABLE I: Wavelength dependence of the deflection angle as a function of applied electric field and linear electro-optic coefficients.

| Wavelength (nm) | Deflection (r_{33}) (mrad•mm/kV) | r_{33} (pm/V) | Deflection (r_{13}) (mrad•mm/kV) | r_{13} (pm/V) |
|--------------------|---|-----------------|---|-----------------|
| 632 | 9.41 | 30.2 | 2.34 | 7.55 |
| 980 | 8.67 | 29.3 | 2.03 | 6.89 |
| 1330 | 7.95 | 27.4 | 1.87 | 6.48 |
| 1558 | 7.78 | 27.1 | 1.96 | 6.84 |

A BPM simulation of the device shown in Fig. 1 predicts a deflection angle per unit field of 9.51 mrad•mm/kV ($n_e=2.180$, $r_{33}=30.5$ pm/V) and 2.55 mrad•mm/kV ($n_o=2.176$, $r_{13}=8.4$ pm/V) for extraordinary and ordinary polarized light, respectively. These values agree with the measured deflection angles per unit field listed in Table I to within 1.1% for r_{33} and within 8.2% for r_{13} . Considering that the uncertainty of the literature values for r_{13} and r_{33} is $\sim 10\%$, this agreement is reasonable [13]. The precision of our technique is estimated at 2% , and therefore may provide a more accurate means of determining electro-optic coefficients than other techniques. Using this excellent agreement between experiment and theory as the basis, and using the wavelength dispersion of refractive index reported in literature for LiTaO₃ [8], the wavelength dispersion of r_{33} and r_{13} at other wavelengths is also calculated (Table I). Note that the values of both r_{33} and r_{13} appear to flatten out at longer wavelengths, which is promising for deflection of even longer wavelength light without a significant decrease in the deflection performance.

CONCLUSION

We have demonstrated efficient electro-optic scanning in the infrared wavelengths using domain patterned ferroelectric LiTaO₃. Using the characteristics of the horn-shaped deflector, we have demonstrated a means of measuring the dispersion of electro-optic coefficients for LiTaO₃ with a relatively simple apparatus. This study indicates that the dispersion in the electro-optic

coefficients decreases at longer wavelengths, and appears to flatten out beyond 1.55 μm , providing important baseline information for device designs in far-infrared applications.

ACKNOWLEDGMENTS

The authors would like to thank N. J. C. Libatique and J. Tafoya of the University of New Mexico for their assistance with the laser sources and experiments. This work was partly supported by funding received by V. Gopalan from the National Science Foundation, and from the Defense Advanced Research Programs Agency-Steered Agile Beams program.

REFERENCES

1. K. T. Gahagan, V. Gopalan, J. M. Robinson, Q. X. Jia, T. E. Mitchell, M. J. Kawas, T. E. Schlesinger, and D. D. Stancil, *Appl. Optics* **38**, 1186 (1999).
2. Q. B. Chen, Y. Chiu, D. N. Lambeth, T. E. Schlesinger, and D. D. Stancil, *J. of Lightwave Tech.* **12**, 1401-1404 (1994).
3. J. Li, H. C. Cheng, M. J. Kawas, D. N. Lambeth, T. E. Schlesinger, and D. D. Stancil, *IEEE Phot. Tech. Lett.* **8**, 1486-1488 (1996).
4. M. Yamada, M. Saitoh, and H. Ooki, *Appl. Phys. Lett.* **69**, 3659-3661 (1996).
5. M. J. Kawas, T. E. Schlesinger, D. D. Stancil, and V. Gopalan, *J. of Lightwave Tech.* **15**, 1716-1719 (1997).
7. K. H. Hellwege and A. M. Hellwege, Eds., *Landolt-Börnstein*, (Springer-Verlag, Berlin, 1981) p. 157-161.
8. F. Gervais and V. Fonseca, in *Handbook of Optical Constants and Solids*, E.D. Palik, Ed., (Academic Press, Boston, 1985), pp. 777-805.
9. V. Gopalan, T.E. Mitchell, *J. Appl. Phys.* **83**, 941-954 (1998).
10. J. C. Fang, M. J. Kawas, J. Zou, V. Gopalan, T. E. Schlesinger, and D. D. Stancil, *IEEE Phot. Tech. Lett.* **11**, 66 (1999).
11. C. Baron, H. Cheng, and M.C. Gupta, *Appl. Phys. Lett.* **68**, 481-483 (1996).
12. C. Baron, H. Cheng, and M.C. Gupta, *Proc. SPIE* **2700**, 118-121 (1996).
13. K. Onuki, N. Uchida, T. Saku, *J. Opt. Soc. Amer.* **62**, 1030 (1972).